Supporting information

Fascinating Tin-Effects on the Enhanced and Large-Current-Density Water Splitting Performance of Sn-Ni(OH)$_2$

Juan Jian,[a] Xianyi Kou,[a] Hairui Wang,[a] Limin Chang,[a,*] Le Zhang,[b] Shuang Gao,[a] Yue Xu[a] and Hongming Yuan[b,*]

[a] Key Laboratory of Preparation and Applications of Environmental Friendly Material of the Ministry of Education, College of Chemistry, Jilin Normal University, Changchun 130103, P. R. China

[b] State Key Laboratory of Inorganic Synthesis and Preparative Chemistry, College of Chemistry, Jilin University, Changchun 130012, Qianjin Street 2699, P. R. China.

[*]**Corresponding authors' E-mails**: changlimin2139@163.com; hmyuan@jlu.edu.cn

Materials used in the experiment:

Pt/C (20 wt %) is obtained from Macklin Ltd. (Shanghai, China), RuO_2 is synthesized from ruthenium chloride hydrate ($RuCl_3 \cdot xH_2O$) purchased from Aladdin Ltd. (Shanghai, China). Nickel foam (NF) is provided by the Li Yuan Technology Co. Ltd. (Shanxi, China). $Na_2SnO_3 \cdot 3H_2O$ is bought from the Aladdin Ltd. (Shanghai, China). H_2NCONH_2, KOH, HCl and other chemicals are supplied by the Beijing chemical reagents company. All the chemicals are analytical pure and do not need the further purification. The NF cannot be directly used until treated by the acid solution (2.0 M HCl) and deionized water.

Experimental instruments:

(1) X-ray diffraction (XRD) patterns were measured by the Rigaku D/Max 2550 X-ray diffract matter (the Cu Kα radiation, λ = 1.5418 Å).

(2) X-ray photoelectron spectroscopy (XPS) was performed on an ESCALAB 250 X-ray photoelectron spectrometer with a monochromatic Al Kα X-ray source (hυ=1486.6 eV). The Au $4f_{7/2}$, Cu $2p_{3/2}$ and Ag $3d_{5/2}$ peak positions were used to calibrate the energy scale of spectrometer, and all binding energies were corrected by the C 1s peak (284.5 eV) corresponding to the C=C bonds. The standard deviation of the binding energy (BE) values was 0.1 eV.

(3) The scanning electron microscopy (SEM) images were provided by JEOL JSM 6700 F electron microscope.

(4) The transmission electron microscopy (TEM) images were obtained with JEM-2100 F microscope, equipped with a field emission gun operating at 200 KV.

(5) The inductively coupled plasma atomic emission spectroscopy (ICP-AES) result was provided by the Perkin-Elmer Optima 3300 DV ICP spectrometer.

(6) The X-ray fluorescence (XRF) result was given by the RIGAKU zsx Primus II, Japan.

(7) Water drop contact angle (CA) experiment was carried out by the contact angle tester (JC-2000CD).

Calculation of the loading mass:

For that the Ni in the $Ni(OH)_2$ comes from the NF, thus, the mass difference before and after the hydrothermal reaction cannot give the certain loading information.

Inspired by the reaction of CH_4N_2S and nickel foam, the S in product Ni_3S_2 comes from CH_4N_2S. We believe that all the O in $Ni(OH)_2$ comes from CH_4N_2O. Therefore, for every 1 mol of $Ni(OH)_2$ produced, 2 mol of CH_4N_2O will be consumed. To make sure the molecular formula of the as synthesized Sn-$Ni(OH)_2$, we assume all the reactants (CH_4N_2O and $Na_2SnO_3{\cdot}3H_2O$) have took part in the reaction. Hence, the mole ratio of CH_4N_2O to $Na_2SnO_3{\cdot}3H_2O$ is 30 : 1, that is, the mole ratio of Ni and Sn is 15 : 1 and the Sn-$Ni(OH)_2$ can be written as $Sn_{0.0625}Ni_{0.9375}(OH)_2$, and its molar mass ($M_{Sn\text{-}Ni(OH)2}$) is 96.44 g mol^{-1}, while $M_{Ni(OH)2}$ is 92.69 g mol^{-1}.

The XRF result (Figure S2) of NF-based Sn-$Ni(OH)_2$ certifies that the mass ratio of Ni and Sn is about 99.35 : 0.65. When the reaction condition are the same, the average evaluated mass for a series of the formed NF-based Sn-$Ni(OH)_2$ is 0.2418 g. Thus, following the XRF data, the mass of Sn in Sn-$Ni(OH)_2$ is $m_{Sn} \approx 0.001572$ g, and the $m_{Sn\text{-}Ni(OH)2} \approx 0.01647$ g. As a result, the $m_{loading} = m_{Sn\text{-}Ni(OH)2} / (1 * 9\ cm^2) \approx 1.83$ mg cm^{-2}.

About the $TOF_{(O2)} = (j * A) / (4 * n * F)$, where "n" is the amount of catalyst substance on the electrode surface that participating in the OER course. Though not all the substance loaded on NF surface took part in the OER process, we still suspect that all of them have participated in the OER course. Therefore, when catalyst with the area (A) of 0.25 cm^2 take part into the reaction, the $n = A * m_{loading} / M_{Sn\text{-}Ni(OH)2}$. Thus, $TOF_{(O2)} \approx j * 0.1366\ cm^2\ C^{-1} = j * 0.1366\ s^{-1}$. For that $TOF_{(H2)} = (j * A) / (2 * n * F)$, hence, $TOF_{(H2)} = j * 0.2732\ s^{-1}$.

Measurement of the Faraday efficiency (FE):

Faraday efficiency (FE) of Sn-$Ni(OH)_2$ for OER can be calculated by the ratio of the amount of O_2 collected by drainage method and the theoretical O_2.

The actual amount O_2 production (labeled as $n_{o\text{-}experimental}$) can be calculated using the equation of $n_{o\text{-}experimental} = V / V_m$, where V is the volume of O_2 collected from the chronoamperometry testing; V_m is molar volume of ideal gas, and $V_m = 22.4$ L mol^{-1}.

For the theoretical O_2 ($n_{o\text{-}theoretical}$) accumulated during the OER. According the OER equation of $4OH^- \rightarrow O_2 + 2H_2O + 4e^-$, where, the electrolytic efficiency (η) can be measured by the equation of $\eta = z * n * F / Q$. Here, "n" is the mole of O_2 generated during the OER, and can be marked as $n_{o\text{-}theoretical}$; "z" is the number of transferred

electrons generated per mole of O_2 during the OER, here, z = 4; "F" is the Faraday constant, F = 96485 C mol^{-1}; "Q" refers to the actual quantity of electric charge, and can be calculated by the flume of Q = Σ i * t. In the chronoamperometry experiment, the Q can be directly calculated.

To evaluate the FE of a catalyst for OER, we assume that 100 % current efficiency occurs during the whole reaction. Hence, η = 1 = 4 * F * $n_{o\text{-}theoretical}$ / Q, therefore, $n_{o\text{-}theoretical}$ = Q / (4 * F).[1-3]

The calculation of density functional theory (DFT):

The spin-polarized density functional theory (DFT) calculations were carried out using the Quantum ESPRESSO.[4] The exchange-correlation functional was described by the Perdew-Burke-Ernzerhof (PBE) parameterization of the generalized gradient approximation (GGA).[5] The interactions between electrons and ions were treated within the projector augmented-wave (PAW) approximation.[6] A cutoff energy of 400 eV was employed for the plane-wave basis set. And a conjugate-gradient algorithm was used to relax the atoms into their instantaneous ground state positions. Besides, the structural optimizations were not stopped until the atomic forces were less than 0.01 eV per Å. The first irreducible Brillouin zone was modeled based on the Gamma-centered scheme, where 6 × 6 × 1 k-point grid was used in geometry optimizations and electronic structure analysis. The vdW-D3 method was adopted to describe the van der Waals interactions.[7] A vacuum of 20 Å width was employed to avoid the interactions between periodic images in the z direction.

The change of the Gibbs free energy (ΔG) for each elementary step at the zero potential can be written as:

$$\Delta G_{(0)} = \Delta E + \Delta E_{ZPE} - T\Delta S$$

Where E is the energy directly obtained from the DFT calculations. E_{ZPE} is the zero-point energy calculated from the equation of E_{ZPE} = 1/2Σhv, in which v is the vibrational frequency of a normal mode; h is the Planck constant; S is the entropy that can be calculated as:[8]

$$S(T) = k_B \sum_i \left(\frac{h\nu_i}{k_B T} \frac{1}{\exp\left(\frac{h\nu_i}{k_B T} - 1\right)} - \ln\left(1 - \exp\left(\frac{h\nu_i}{k_B T} - 1\right)\right) \right)$$

k_B and v_i are the Boltzmann constant and vibrational frequency, respectively.

Considering OER mainly processing follow four-steps:

$OH^- + * \rightarrow *OH + e^-$ (1)

$*OH + OH^- \rightarrow *O + H_2O + e^-$ (2)

$OH^- + *O \rightarrow *OOH + e^-$ (3)

$*OOH + OH^- \rightarrow O_2 + H_2O + * + e^-$ (4)

When forming one molecule of O_2 in the reaction step, the reaction free energy can be expressed as $\Delta G_{(2H2O \rightarrow O2+2H2)} = 4.92$ eV $= E_{O2} + 2E_{H2} - 2E_{H2O} + (\Delta ZPE - T\Delta S)_{(2H2O \rightarrow O2+2H2)}$. Hence, the reaction free energy of each step can be expressed as follows:

$\Delta G_{(1)} = E_{(*OH)} - E_{(*)} - E_{H2O} + 1/2\ E_{H2} + (\Delta ZPE - T\ \Delta S)_{(1)}$ (5)

$\Delta G_{(2)} = E_{(*O)} - E_{(*OH)} + 1/2\ E_{H2} + (\Delta ZPE - T\ \Delta S)_{(2)}$ (6)

$\Delta G_{(3)} = E_{(*OOH)} - E_{(*O)} - E_{H2O} + 1/2\ E_{H2} + (\Delta ZPE - T\ \Delta S)_{(3)}$ (7)

$\Delta G_{(4)} = E_{(*)} - E_{(*OOH)} + E_{O2} + 1/2\ E_{H2} + (\Delta ZPE - T\ \Delta S)_{(4)}$ (8)

where $E_{(*)}$, $E_{(*OH)}$, $E_{(*O)}$, and $E_{(*OOH)}$ are the computed DFT energies of the pure surface and the adsorbed surfaces with *OH, *O and *OOH, respectively. E_{H2O}, E_{H2} and E_{O2} are the computed energies for the sole H_2O, H_2 and O_2 molecules, respectively. As a result, the reaction overpotential can be obtained by evaluating the difference between the minimum voltage needed for the OER.

As for the HER ($H^* + e^- \rightarrow 1/2\ H_2$), the HER catalytic activities are evaluated by computing the ΔG_{H^*} values of possible catalytic sites according to the equation:

$\Delta G_{H^*} = \Delta E_{H^*} + \Delta ZPE - T\Delta S$ (9)

In addition, the binding energy of H_2O is calculated as formula:

$\Delta E_{ads} = E_{substrate+H2O} - E_{substrate} - E_{H2O}$ (10)

where $E_{substrate+H2O}$, $E_{substrate}$, and E_{H2O} are the total energies of the whole system, the substrate, and the gas phase H_2O molecule, respectively.

Supplementary Figures

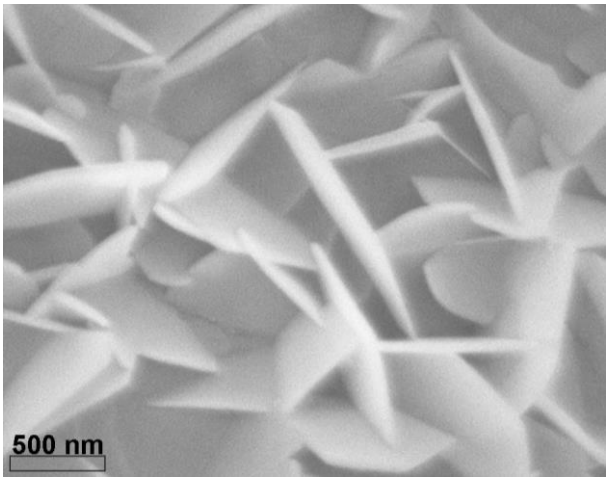

Figure S1. The SEM image of pure $Ni(OH)_2$.

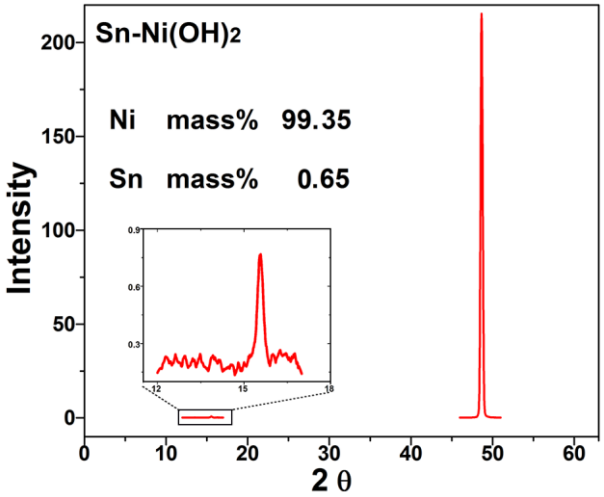

Figure. S2. The X-ray fluorescence (XRF) result of Ni and Sn in the Sn-$Ni(OH)_2$, insert picture is the magnified image of the curves at 2θ range of 12 ~ 18°. Note, the range (R) of the XRF data is 0.00139, R% = 1.39.

Table S1. The ICP-AES results of Sn and Ni in the Sn-$Ni(OH)_2$, concentration of the standard solution is 10 mg mL^{-1}.

Elements	Ni_{2316}	Sn_{1899}
Average content (ppm)	241.8	0.2849
Standard deviation (SD)	6.3	0.0008
% RSD	2.605	0.2808

Note, ppm refers to the mass concentration, and is the abbreviation of part per million.

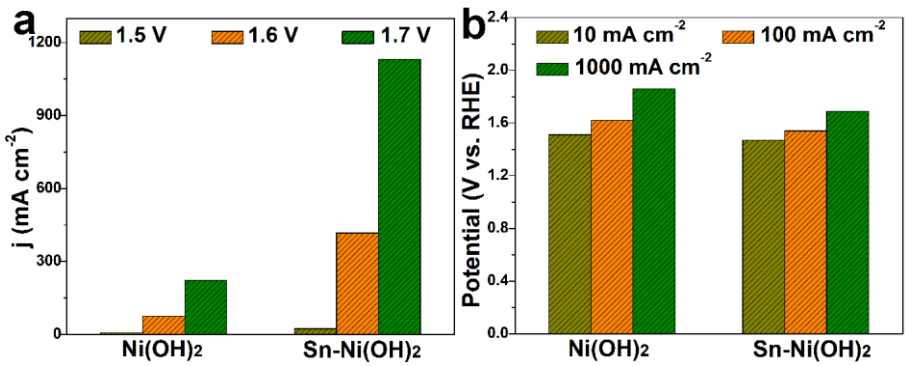

Figure S3. The bar graphs between a) potentials and b) current densities of $Ni(OH)_2$ and Sn-$Ni(OH)_2$ for OER.

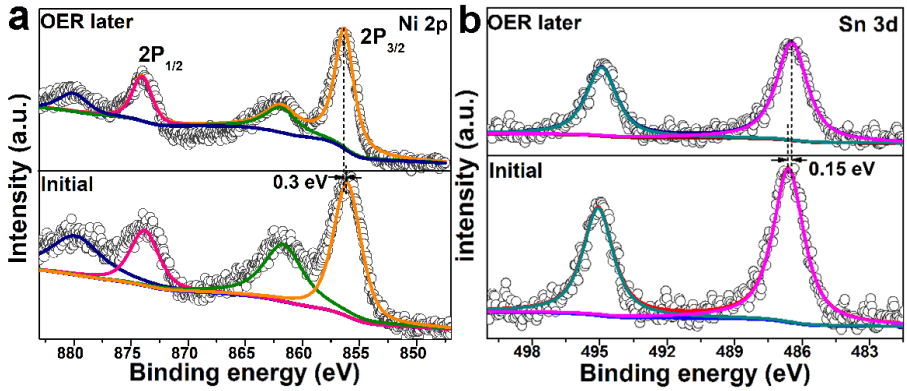

Figure S4. The XPS results of a) Ni 2p, b) Sn 3d of Sn-$Ni(OH)_2$ after the OER.

As shown in the Figure S4, after the OER process, both the Ni 2p and the Sn 3d have some difference with the initial ones, the corresponding spectrum shift of 0.3 eV and -0.15 eV, respectively, certifies the strong electronic intercalation between Ni and Sn.

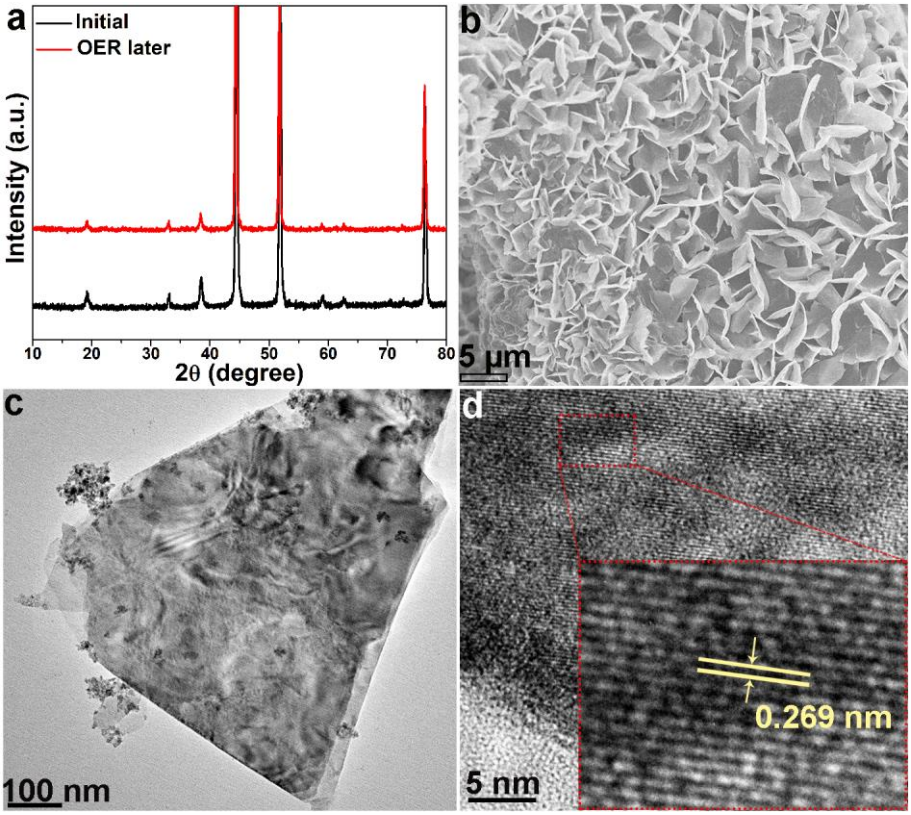

Figure S5. The a) XRD results, b) SEM and c,d) HRTEM images of Sn-$Ni(OH)_2$ after OER.

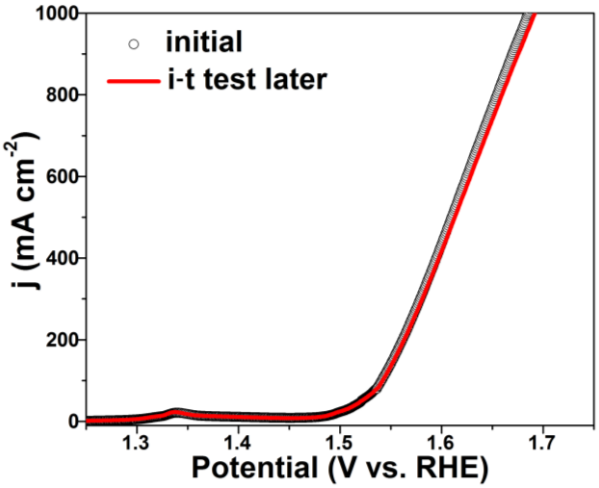

Figure S6. The LSV curves before (black) and after (red) the i-t test.

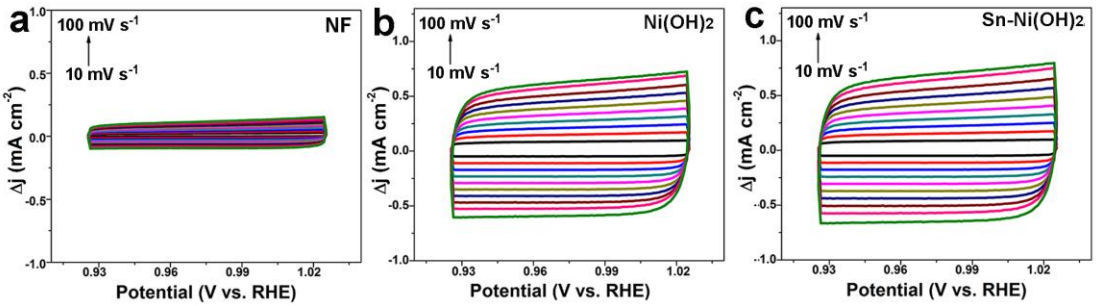

Figure S7. The CV curves of a) NF, b) $Ni(OH)_2$, c) Sn-$Ni(OH)_2$ with different scan rates at the range of 0.9254-1.0254 V (vs. RHE).

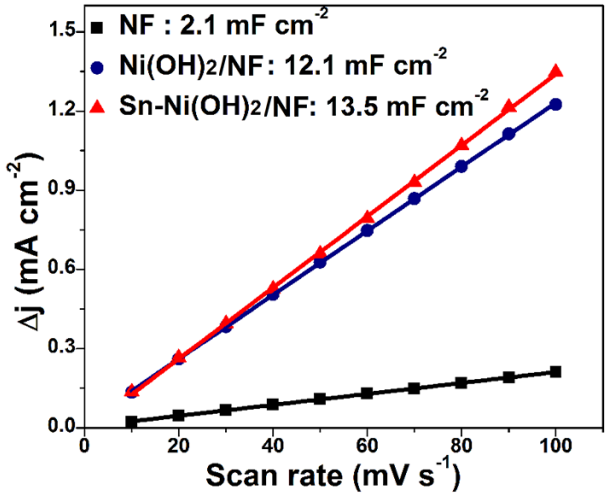

Figure S8. The corresponding fitted slope curves of NF (black), $Ni(OH)_2$ (blue) and Sn-$Ni(OH)_2$ (red).

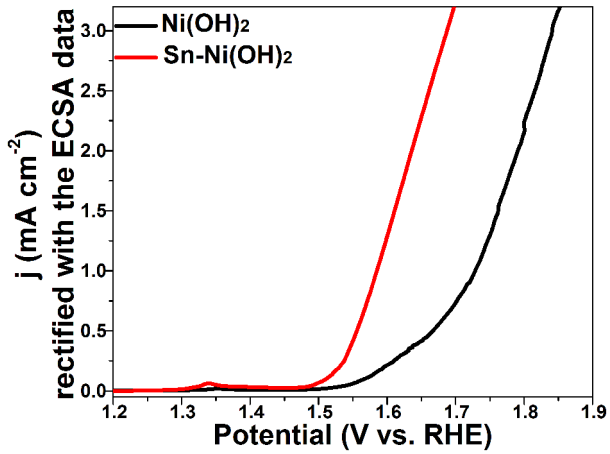

Figure S9. The LSV curves of Sn-$Ni(OH)_2$ (red) and $Ni(OH)_2$ (black) that rectified with the ECSA data.

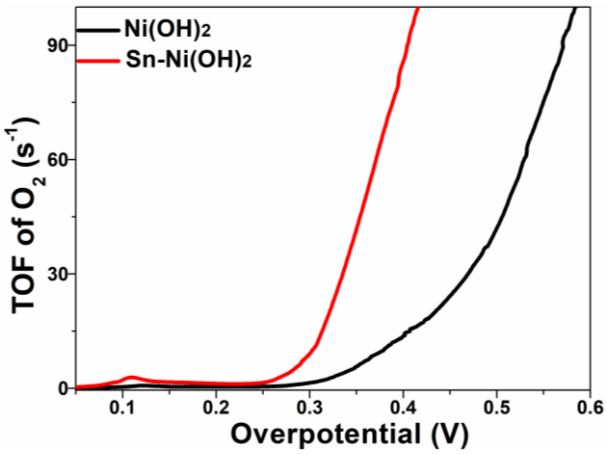

Figure S10. The TOF of O_2 curves for Sn-Ni(OH)$_2$ (red) and Ni(OH)$_2$ (black).

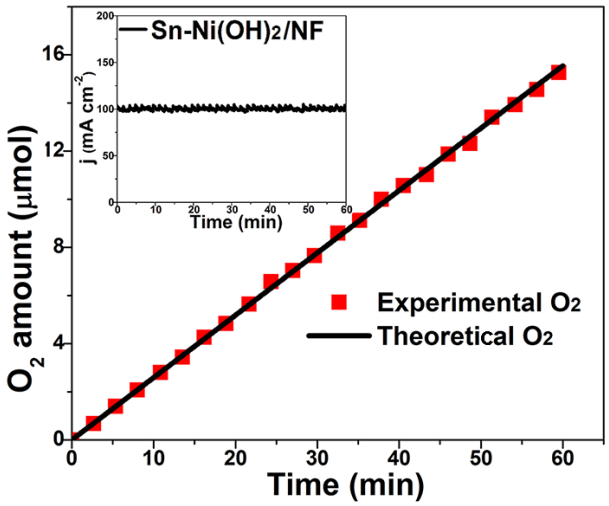

Figure S11. The relationship between time and the generated O_2 (both experimental and theoretical) during the OER course, insert is the corresponding i-t curves.

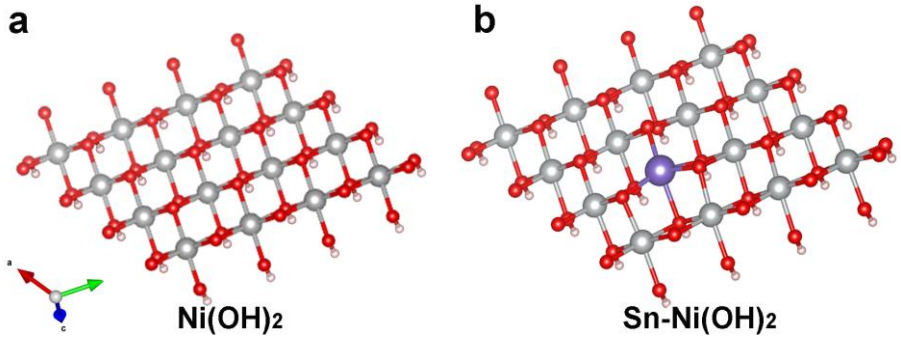

Figure S12. The slab models of the a) Ni(OH)$_2$, and b) Sn-Ni(OH)$_2$ system. Noted, the sphere of gray, purple, red and pink are referred to the Ni, Sn, O and H atoms, respectively (In order to make the image more intuitive, the top H is ignored).

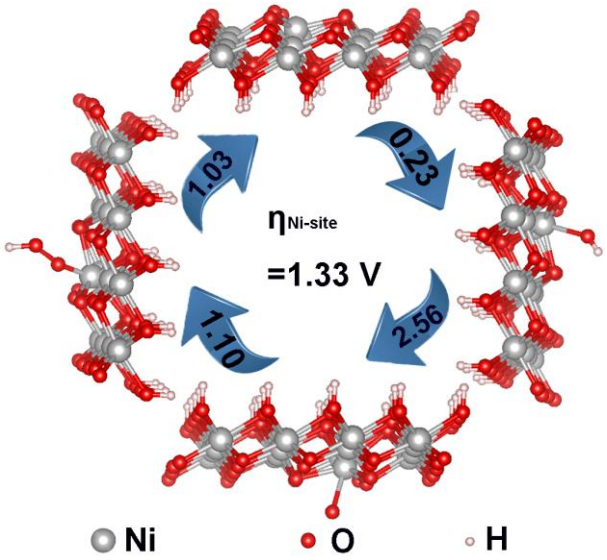

Figure S13. The optimized structures of *OH, *O, and *OOH adsorptions of $Ni(OH)_2$ during the OER process. Note that the gray, red and pink spheres represent Ni, O and H atoms, respectively.

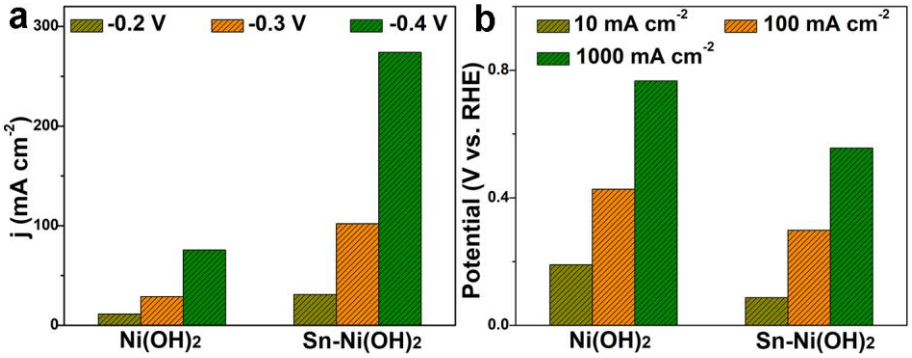

Figure S14. The bar graphs between a) potentials and b) current densities of $Ni(OH)_2$ and Sn-$Ni(OH)_2$ for HER.

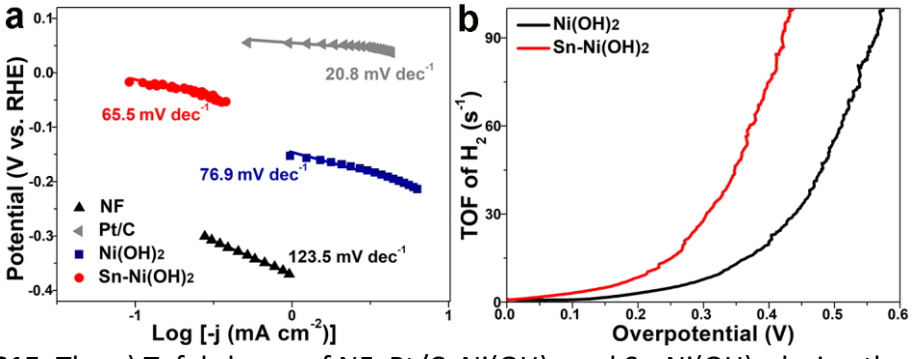

Figure S15. The a) Tafel slopes of NF, Pt/C, $Ni(OH)_2$ and Sn-$Ni(OH)_2$ during the HER, b) TOF of H_2 curves for Sn-$Ni(OH)_2$ (red) and $Ni(OH)_2$ (black).

As shown in Figure S15a, Sn-$Ni(OH)_2$ has lower Tafel slope data than the undoped $Ni(OH)_2$, demonstrating that the current density of Sn-$Ni(OH)_2$ changes faster with

voltage, that is, it has a faster reaction kinetics than the $Ni(OH)_2$. In addition, in alkaline electrolyte, HER mainly follow the steps below:[9]

Volmer step: $H_2O + * + e^- \rightarrow H^* + OH^-$ (120 mV dec^{-1})

Heyrovsky step: $H^* + H_2O + e^- \rightarrow H_2 + OH^-$ (40 mV dec^{-1})

Or, Tafel step: $2H^* \rightarrow H_2$ (30 mV dec^{-1}).

Hence, Tafel slope value of Sn-$Ni(OH)_2$ confirms that during the HER course, Sn-$Ni(OH)_2$ occurs via a Volmer-Heyrovsky mechanism, in which the recombination of adsorbed H atom with H_2O is the rate-determining step.[10]

Table S2. Comparation of some recently reported OER electrocatalysts.

Catalysts	$\eta_{10\ mA\ cm-2}$ (mV)	$\eta_{100\ mA\ cm-2}$ (mV)	$\eta_{1000\ mA\ cm-2}$ (mV)	Reference
Sn-Ni(OH)$_2$	**246**	**312**	**460**	**This work**
Ni(OH)$_2$	**290**	**396**	**630**	**This work**
RuO$_2$	**260**	**340**	**710**	**This work**
P-MoS$_2$@CoP	282	—	—	ChemSusChem 2021, 14, 1565-1573
NiFeW/NF	224	266	—	ChemSusChem 2021, 14, 1324-1335
Co$_3$Mo/Cu	$\eta_{onset} \approx 261$	≈ 330	—	Nat. Commun. 2020, 11, 2940
W-Ni(OH)$_2$/NF	237	—	—	Nat. Commun. 2019, 10, 2149
MoS$_2$-NiS$_2$/NGF	≈ 370	—	—	Appl. Catal., B, 2019, 254, 15
Co/CNFs	320	≈ 450	—	Adv. Mater. 2019, 31, 1808043
CuCoS nanosheets	310	—	—	ACS Catal. 2017, 7, 5871-5879
NiPS$_3$ nanosheets	294	≈ 370	—	ACS Nano 2018, 12, 5297-5305
CoS$_x$/NGF	315	—	—	ACS Nano 2018, 12, 12369-12379
NiFe-LDH/NF	300	—	—	Nat. Commun. 2014, 5, 4477
NiCoFe-LDH/NF	340	—	—	Adv. Energy Mater. 2015, 5, 500245
CoFePO/NF	274.5	≈ 410	—	ACS Nano 2016, 10, 8738
RuO$_2$/NiO/NF	250	≈ 330	—	Small 2018, 14, 1704073
Fe-Ni$_3$S$_2$/FeNi	282	≈ 470	—	Small 2017, 13,

				1604161
Fe-NiSe/NF	233	275	—	J. Mater. Chem. A, 2017, 5, 14639
CoMoO/NF	270	330	—	Nano energy 2018,45,448
P-CoNiS/NF	292.2	≈ 300	≈ 440 (@500 mA cm^{-2})	ACS Appl. Mater. Interfaces 2018, 10, 7087
$NiOOH/Ni(OH)_2$	390.5	—	—	ChemSusChem 2019, 12, 1469
Ni_3Fe/N-C sheets	390	≈ 320	—	Adv. Energy Mater. 2017, 7, 1
CoS_x/Ni_3S_2@NF	280 (@20 mA cm^{-2})	≈ 390	—	ACS Appl. Mater. Interfaces 2018, 33, 27712
NiFe-LDH/Fe-N-C	310	—	—	Energy Environ. Sci., 2016, **9**, 2020

Table S3. The fitted slopes, double-layer-capacitance (C_{dl}) and corresponding electrochemical surface area (ECSA) results of $Ni(OH)_2$ and Sn-$Ni(OH)_2$.

Elements	**NF**	**$Ni(OH)_2$**	**Sn-$Ni(OH)_2$**
Fitted slope (mF cm^{-2})	4.2	24.2	27.0
Standard error for slope	6.97×10^{-6}	4.04×10^{-5}	8.02×10^{-5}
Double-layer-capacitance (C_{dl}, mF cm^{-2})	2.1	12.1	13.5
Electrochemical surface area (ECSA, cm^2)	13.12	75.62	84.38

Note, ECSA = A * C_{dl} / C_s, here, A = 0.25 cm^2, C_s = 0.04 mF cm^{-2}.

Table S4. Comparation of some recently reported HER electrocatalysts.

Catalysts	$\eta_{10\ mA\ cm-2}$ (mV)	$\eta_{100\ mA\ cm-2}$ (mV)	$\eta_{1000\ mA\ cm-2}$ (mV)	Reference
Sn-Ni(OH)$_2$	**87**	**298**	**556**	**This work**
Ni(OH)$_2$	**190**	**427**	**767**	**This work**
Pt/C	**20.6**	**184**	——	**This work**
N, B-Ni$_2$P/G	124	——	——	Appl. Catal. B: Environ. 2020, **278**, 119284
RhSe$_2$	81.6	——	——	Adv. Mater. 2021, **33**, 2007894
Au/CoP@NC-3	140.9	——	——	ACS Appl. Mater. Interfaces 2020, **12**, 16548-16556
P-CoS$_2$/Ti	91	——	——	Nanoscale 2020, **12**, 11573-11581
P-MoS$_2$@CoP	64	141	458	ChemSusChem 2021, 14, 1565-1573
H-MoS$_2$/MoP	92	——	——	Small 2020, 2002482
Co/CNFs	190	——	——	Adv. Mater., 2019, **31**, 1808043
CoFeZr oxides/NF	104	≈230	——	Adv. Mater., 2019, 1901439
CoFe@NiFe/NF	240	≈340	——	Appl. Catal., B, 2019, **253**, 131
Co$_9$O$_8$/Ni$_3$S$_2$/NF	128	≈230	——	Appl. Catal., B, 2019, **253**, 246
MoS$_2$-NiS$_2$/NGF	172	——	——	Appl. Catal., B, 2019, **254**, 15
Ni doped graphitic carbon (NGC)	220	≈580	——	Carbon, 2019, **150**, 21
NiOOH/Ni(OH)$_2$	147	——	——	ChemSusChem, 2019, **12**, 1469

CoMoP nanosheet arrays@NF	173	≈305	——	Nano Energy, 2018, **45**, 448
Ni_3FeN/r-GO	94	≈200	——	ACS Nano, 2018, **12**, 245
P-Co_3O_4/NF	97	——	——	ACS Catal., 2018, **8**, 2236
CoP@3D Ti_3C_2-MXene	168	——	——	ACS Nano, 2018, **12**, 8017
Co/$Co_2Mo_3O_8$/NF	25	≈210	——	ACS Catal., 2018, **8**, 5062
P-doped CoNiS/NF	187.4	≈220	≈240 (500 $mAcm^{-2}$)	ACS Appl. Mater. Interfaces, 2018, **10**, 7087
N-doped Ni_3S_2 nanosheets	155	≈320	——	Adv. Energy Mater., 2018, **8**, 1703538
Sn-Ni_3S_2/NF	35	170	570	ACS Appl. Mater. Interfaces, 2018, **10**, 40568
Ni_2P-Ni_3S_2 HNAs/NF	80	≈180	——	Nano Energy, 2018, **51**, 26
N-Ni_3S_2/ NF	110	≈250	——	Adv. Mater., 2017, **29**, 1701584
Cu@CoS_x/Cu Foam	134	267	——	Adv. Mater., 2017, **29**, 1606200

Table S5. Comparation of some recently reported OWS electrocatalysts.

Catalysts	$E_{10\ mA\ cm^{-2}}$ (V)	$E_{100\ mA\ cm^{-2}}$ (V)	Reference
Sn-$Ni(OH)_2$‖Sn-$Ni(OH)_2$	**1.58**	**1.87**	**This work**
$Ni(OH)_2$‖$Ni(OH)_2$	**1.65**	**2.03**	**This work**
Pt/C‖RuO_2	**1.57**	**1.84**	**This work**
Nano-KFO/NF	1.59	1.73	J. Mater. Chem. A, 2021, **9**, 7586-7593
P-MoS_2@CoP	——	1.68	ChemSusChem 2021, **14**, 1565-1573
Co_3Mo/Cu	——	1.62	Nat. Commun. 2020, 11, 2940
Co-MOF/H_2	1.619	——	Nanoscale 2020, **12**, 8969.
Co/CNFs	1.60	——	Adv. Mater., 2019, **31**, 1808043
CoFeZr oxides/NF	1.63	≈1.80	Adv. Mater., 2019, 1901439
CoFe@NiFe/NF	1.59	——	Appl. Catal., B, 2019, **253**, 131
Co_9S_8/Ni_3S_2/NF	1.64	——	Appl. Catal., B, 2019, **253**, 246
MoS_2-NiS_2/NGF	1.64	——	Appl. Catal., B, 2019, **254**, 15
Ni doped graphitic carbon (NGC)	1.64	——	Carbon, 2019, **150**, 21
CoMoO nanosheet arrays@NF	1.68	≈1.88	Nano Energy, 2018, **45**, 448
Ni_3FeN/r-GO	1.60	≈1.96	ACS Nano, 2018, **12**, 245
P-Co_3O_4/NF	1.63	——	ACS Catal., 2018, **8**, 2236
CoP@3D Ti_3C_2-MXene	1.57	≈1.70	ACS Nano, 2018, **12**, 8017

P-doped Co-Ni-S/NF	1.60	——	ACS Appl. Mater. Interfaces, 2018, **10**, 7087
NiFe/$Ni(OH)_2$/NiAl	1.59	——	Adv. Sci., 2017, **4**, 1700084
Ni_3S_2-NGQDs/NF	1.58	——	Small, 2017, **13**, 1700264
N(P)-doped 304-type stainless steel mesh	1.74	——	Adv. Mater., 2017, 1702095

References for the supporting information:

[1] Liu, Y. P.; Zou, X. X. et al, *Nat. Commun.* **2018**, 9, 2609.

[2] Suryanto, B. H. R.; Zhao, C. et al, *Nat. Commun.* **2019**, 10, 5599.

[3] Zou, X. X.; Zhang Y. *Chem. Soc. Rev.*, **2015**, 44, 5148-5180.

[4] Giannozzi, P.; Baroni, S. et al. *J. Phys. Condens. Matter* **2009**, 21, 395502.

[5] J. P. Perdew, K. Burke and M. Ernzerhof, *Phys. Rev. Lett.*, **1996**, *77*, 3865.

[6] P. E. Blöchl, *Phys. Rev. B: Condens. Matter Mater. Phys.*, **1994**, *50*, 17953-17979.

[7] S. Grimme, J. Antony, S. Ehrlich and H. Krieg, *J. Chem. Phys.*, **2010**, *132*, 154104.

[8] Björk, *J. Phys. Chem. C*, **2016**, *120*, 21716-21721.

[9] Liu, B. Z.; Peng, Y. et al, *Nat. Commun*. **2019**, 10, 631.

[10] Chen, H.; Ai, X.; Zou, X. X. et al. *Angew. Chem. Int. Ed.* **2019**, 58, 1-6.